

## Supporting Information for

# A new reductant in gold cluster chemistry gives a superatomic gold gallium cluster.

Florian Fetzler,<sup>a</sup> Claudio Schrenk,<sup>a</sup> Nia Pollard,<sup>b,c</sup> Adebola Adeagbo,<sup>b</sup> Andre Z. Clayborne,<sup>\*b</sup>  
Andreas Schnepf<sup>\*a</sup>

a) Institute of Inorganic Chemistry, Universität Tübingen, Auf der Morgenstelle 18, D-72076  
Tübingen, Germany.

b) Department of Chemistry, Howard University, 525 College Street NW, Washington,  
District of Columbia, United States of America.

c) Department of Chemistry and Biochemistry, George Mason University, 4400 University  
Drive MSN 3E2, Fairfax, Virginia, United States of America.

1. Experimental Details .....	2
2. NMR data of $[(PPh_3)_8Au_9GaCl_2]^{2+}$ .....	3
3. Crystal data .....	6
4. Computational Details .....	6
5. Detailed View of $[(PPh_3)_8Au_9GaCl_2]^{2+}$ and $[(PMe_3)_8Au_9GaCl_2]^{2+}$ .....	8
6. Optical spectra of <b>1</b> and <b>1<sub>Me</sub></b> .....	8
7. Electron density corresponding to optical transitions .....	9
8. TGA measurements .....	11
9. HR-ESI-MS spectra .....	11

# 1. Experimental Details

All reactions were carried out under standard Schlenk techniques. THF, diethyl ether and toluene were degassed, dried with sodium and purified via distillation.

NMR spectroscopy was performed on a Bruker AVIIIHD-300 spectrometer. The chemical shifts are given in ppm against the external standards SiMe<sub>4</sub> (<sup>1</sup>H, <sup>13</sup>C,) and 85% phosphoric acid (<sup>31</sup>P).

Mass spectroscopy has been performed on a maXis 4G from Bruker Daltonic.

Elemental analysis was performed on an Elementar vario MICRO cube.

TGA measurements were executed on a NETZSCH STA449 F3 Jupiter heating the samples with 2 K/min starting at 28°C up to the final temperature of 1080°C.

## **Synthesis of [(PPh<sub>3</sub>)<sub>8</sub>Au<sub>9</sub>GaCl<sub>2</sub>]<sup>2+</sup>**

GaCp was prepared according to the literature.<sup>1</sup> The freshly prepared GaCp solution (1 mmol in 10 ml of toluene) was decanted onto a solution of PPh<sub>3</sub>AuCl (498 mg, 1 mmol) in 10 ml of toluene. The clear solution initially turned yellow before taking on a reddish to orange colour in the progress of the reaction. The reaction was allowed to stir for 12 hours leading to a precipitation of a dark solid. The solvent was removed under reduced pressure and the residual solid was dissolved in THF. Addition of 3 ml of diethyl ether lead to the formation of black crystals suitable for single crystal X-ray analysis. (yield: 93 mg, 0.19 mmol, 19.2% in respect to gold)

**$^1\text{H}$  NMR** (300 MHz, DCM- $d_2$ ):  $\delta = 6.04$  (s, 5.6 H,  $\text{C}_5\text{H}_5$ ), 6.7 (m, Ph), 6.8 (m, Ph), 7.08 (m, Ph), 7.18 (m, Ph), 7.33 (m, Ph) ppm.

**$^{31}\text{P}\{^1\text{H}\}$  NMR** (121 MHz, DCM- $d_2$ ):  $\delta = 56.03$  (s).

## 2. NMR data of $[(\text{PPh}_3)_8\text{Au}_9\text{GaCl}_2]^{2+}$

The following spectrum shows the  $^{31}\text{P}$ -signals for the title compound  $[(\text{PPh}_3)_8\text{Au}_9\text{GaCl}_2]^{2+}$  at 56 ppm along with minor impurities. The integration of the signals yield impurities of 14%.

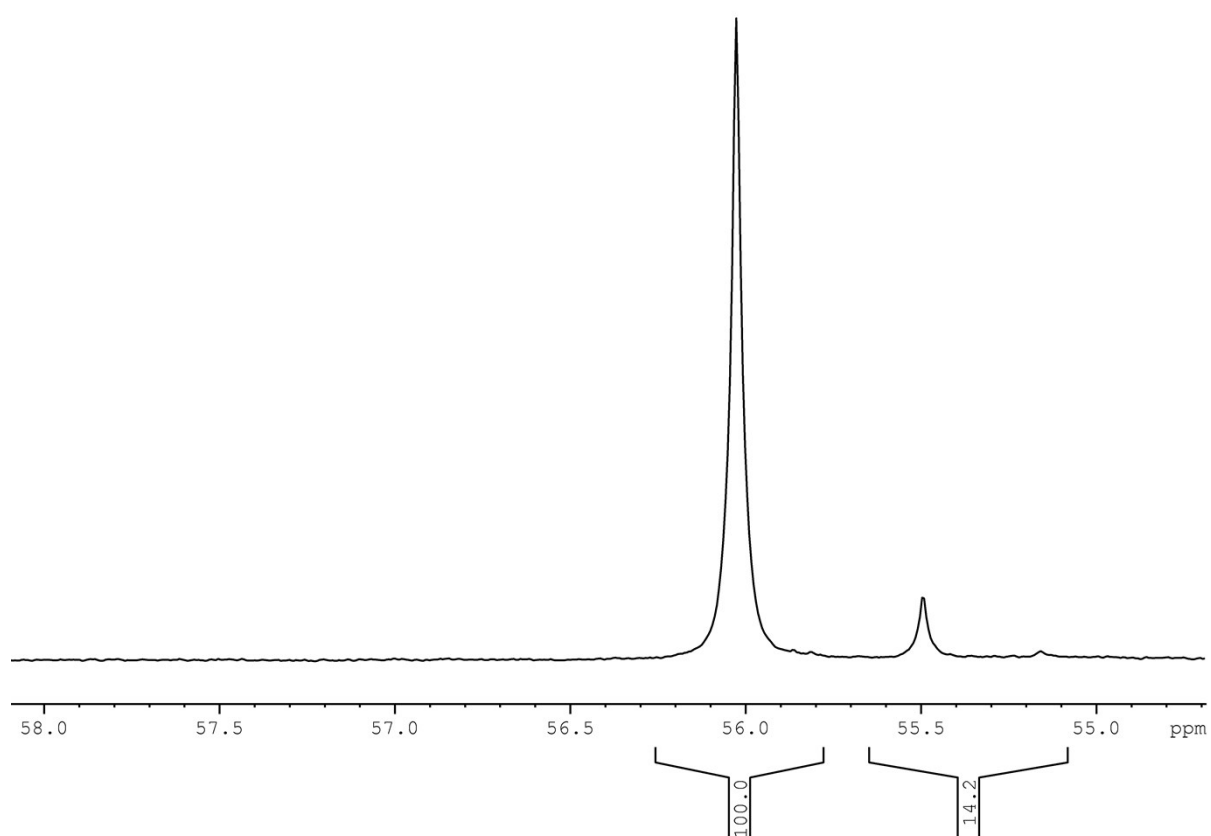


Figure S1:  $^{31}\text{P}$ -NMR-spectrum of the title compound **1** in dichloro-methane. The main signal at 56 ppm refers to the main product. Impurities can be calculated to 14%.

These impurities are caused by degradation of the title compound in solution over time as revealed by NMR after keeping the probe in solution for 24 h (Figure S2).

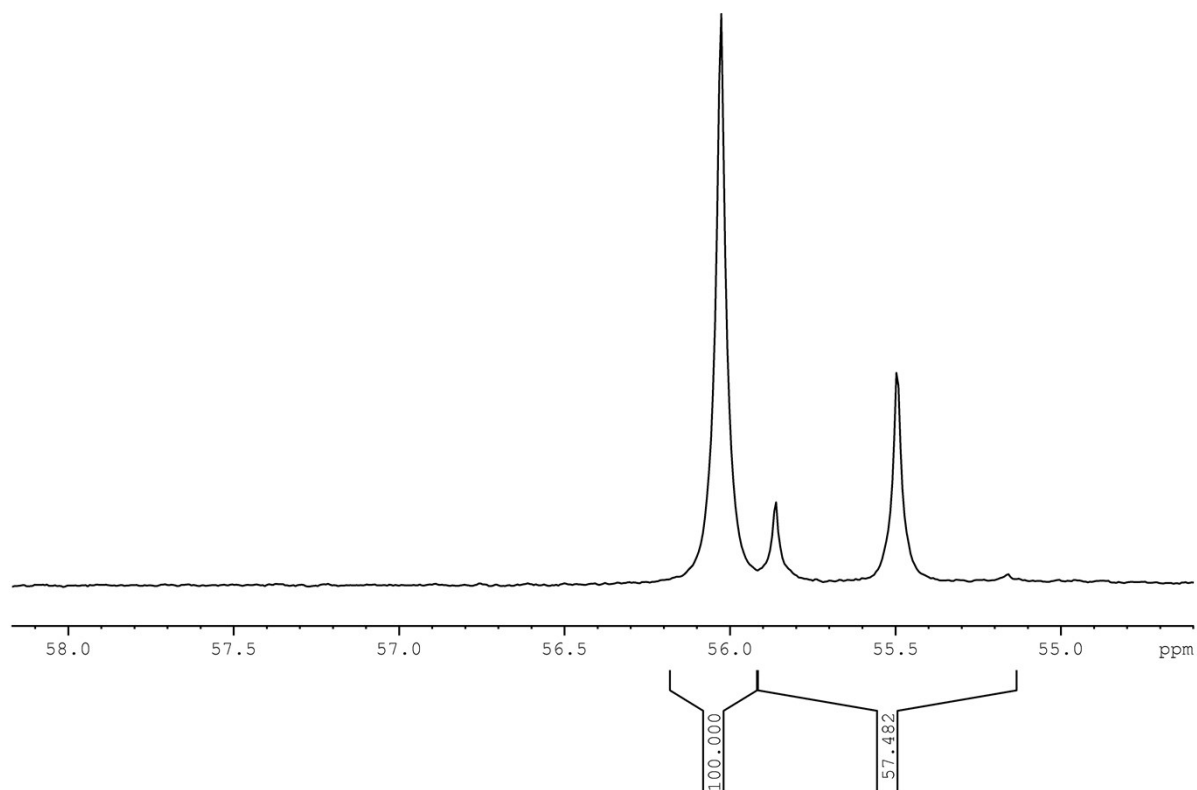
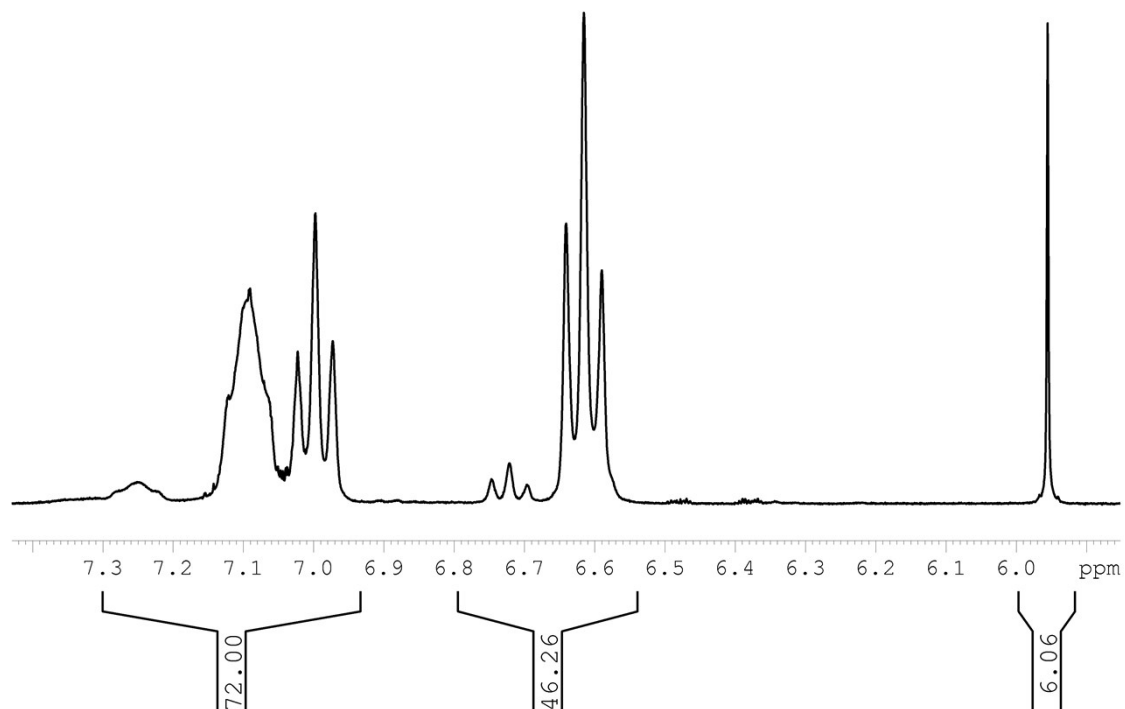


Figure S2:  $^{31}\text{P}$ -NMR-spectrum of the title compound **1** in dichloro-methane after 24 hours in solution. The main signal at 56 ppm refers to the main product. An increase of the impurities can be observed due to degradation in solution over time.

To confirm the composition of the anions found in the single crystal X-ray analysis the  $^1\text{H}$ -NMR-spectrum was analyzed. (Figure S3) The peaks at 6.6-6.8 ppm and 7.1-7.4 ppm correlate to the 120 protons of the aromatic phenyl groups of the main compound. The integral of the peak at about 6 ppm correlates to the cyclopentadiene group at the anion  $\text{GaCpCl}_3^-$ . The integral correlates to 6 hydrogen atoms which calculates into 1.2 cyclopentadienyl groups which is consistent with the anion ratio  $\text{GaCpCl}_3^- : \text{GaCl}_4^-$  of 60:40 found in the single crystal X-ray analysis. The three main signals at 6.6 ppm, 7.0 ppm and 7.1

ppm correlate to the hydrogen atoms of the main product while the smaller signals at 6.7 and 7.25 ppm correlate to the impurities caused by the degradation in solution.



**Figure S3:**  $^1\text{H}$ -NMR-spectrum of  $[(\text{PPh}_3)_8\text{Au}_9\text{GaCl}_2]^{2+}$  in dichloro-methane. The peaks at 6.6 – 7.4 ppm correlate to the aromatic phenyl groups of the tri-phenyl-phosphine ligands. The peak at about 6 ppm correlates with the hydrogen atoms at the cyclopentadiene groups.

### 3. Crystal data

Crystals were mounted on the diffractometer at 150 K. The data were collected on a Bruker APEX II DUO diffractometer equipped with an I $\mu$ S microfocus sealed tube and QUAZAR optics for monochromated MoK $\alpha$  radiation ( $\lambda = 0.71073 \text{ \AA}$ ) and equipped with an Oxford Cryosystems cryostat. A semiempirical absorption correction was applied using the program SADABS. The structure was solved by direct methods and refined against  $F^2$  for all observed reflections. Programs used: SHELXT and SHELXL<sup>[2]</sup> within the Olex2 program package.<sup>[3]</sup>

The cationic cluster  $[(\text{PPh}_3)_8\text{Au}_9\text{GaCl}_2]^{2+}$  could be refined properly, the anions are refined as a superposition of  $\text{GaCl}_4^-$  and  $\text{CpGaCl}_3^-$  in the ratio 40:60, as monitored by NMR (*vide infra*).

The program routine SQUEEZE<sup>[4]</sup> which is implemented in the program routine PLATON was used to model non-refineable solvent molecules. So, one void per molecule is found, containing 147 electrons in a volume of  $527 \text{ \AA}^3$ . This fits to 3.5 solvent molecules ( $\text{Et}_2\text{O}$ , THF – both have almost the same number of electrons), which can both be found in the NMR spectrum.

The H atom positions in all compounds were refined using a riding model. The supplementary crystallographic data (CCDC numbers: 2032544) can be obtained online free of charge at [www.ccdc.cam.ac.uk/conts/retrieving.html](http://www.ccdc.cam.ac.uk/conts/retrieving.html) or from Cambridge Crystallographic Data Centre, 12 Union Road, Cambridge CB21EZ; Fax: (+44)1223-336-033; or [deposit@ccdc.cam.ac.uk](mailto:deposit@ccdc.cam.ac.uk).

Empirical formula	$C_{150.23}H_{126.23}Au_9Cl_{8.76}Ga_3P_8$
Formula weight	4471.45
Temperature/K	150.0
Crystal system	monoclinic
Space group	C2/c
a/Å	31.0956(13)
b/Å	15.1623(6)
c/Å	33.4620(14)
$\alpha/^\circ$	90
$\beta/^\circ$	97.4410(10)
$\gamma/^\circ$	90
Volume/Å <sup>3</sup>	15643.8(11)
Z	4
$\rho_{\text{calc}}/\text{g/cm}^3$	1.899
$\mu/\text{mm}^{-1}$	9.188
F(000)	8402.0
Crystal size/mm <sup>3</sup>	0.274 × 0.194 × 0.061
Radiation	MoK $\alpha$ ( $\lambda = 0.71073$ )
2 $\theta$ range for data	3.3 to 48.99
Index ranges	$-36 \leq h \leq 36, -17 \leq k \leq 17, -39 \leq l \leq 39$
Reflections collected	81808
Independent reflections	13018 [ $R_{\text{int}} = 0.0702, R_{\text{sigma}} = 0.0487$ ]
Data/restraints/parameters	13018/130/857
Goodness-of-fit on F <sup>2</sup>	1.092
Final R indexes [ $I \geq 2\sigma(I)$ ]	$R_1 = 0.0451, wR_2 = 0.1009$
Final R indexes [all data]	$R_1 = 0.0672, wR_2 = 0.1149$
Largest diff. peak/hole / e Å <sup>-3</sup>	2.81/-1.20
CCDC number	2032544

## 4. Computational Details

First principle density functional calculations were carried out using GPAW.<sup>[5]</sup> The electron wavefunctions were projected onto a real-space grid with a grid spacing of 0.20 Å with 7.0 Å of vacuum surrounding each system. The exchange and correlation effects were accounted for through the Perdew, Burke, and Ernzerhof (PBE)<sup>[6]</sup> functional. Structure optimization calculations were performed with a maximal force of 0.05 eV/Å to ensure ground-state energy

configurations were achieved. The structural relaxation was performed for two structures,  $\text{Au}_9(\text{PPh}_3)_8\text{GaCl}_2^{2+}(\mathbf{1})$  and  $\text{Au}_9(\text{PMe}_3)_8\text{GaCl}_2^{2+}(\mathbf{1}_{\text{Me}})$ . Table S1 shows the difference in bond lengths between the computed ground state structures and the crystal structure. Visualization of the electron density was rendered using VESTA.<sup>7</sup>

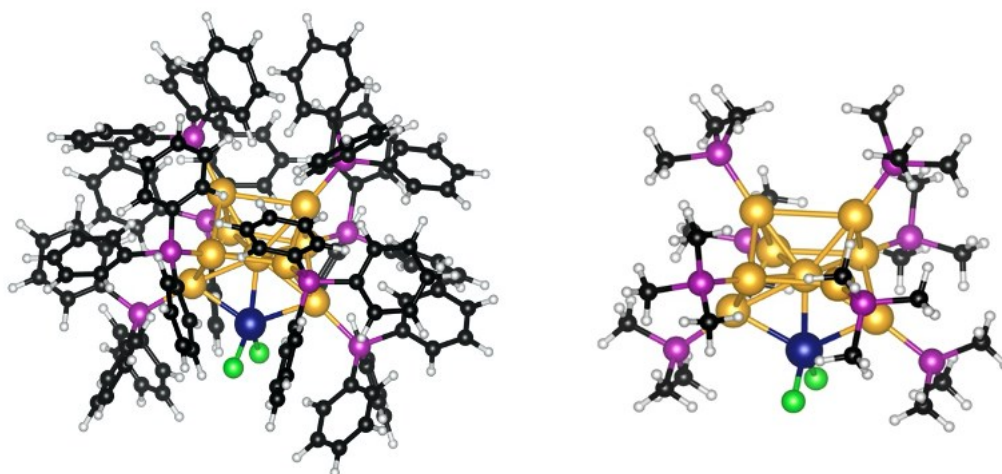
**Table S1.** Comparison of bond lengths (Å) between the relaxed structures ( $\mathbf{1}$  and  $\mathbf{1}_{\text{Me}}$ ) and the unrelaxed (crystal) structure of  $\text{Au}_9(\text{PR}_3)_8\text{GaCl}_2^{2+}$ .

Bonds	$\text{Au}_9(\text{PPh}_3)_8\text{GaCl}_2^{2+}$	$\text{Au}_9(\text{PMe}_3)_8\text{GaCl}_2^{2+}$	Experimental
Au-Au	2.90	2.89	2.82
Au-Ga	2.65	2.65	2.61
Au-P	2.36	2.33	2.30
Ga-Cl	2.26	2.25	2.21

The simulated optical spectra were obtained using linear response-time dependent density functional theory (Lr-TDDFT)<sup>[8]</sup> module as implemented in GPAW using the PBE functional. For the Lr-TDDFT calculations, we changed the grid spacing to 0.25 Å. We obtained an optical spectrum for  $\mathbf{1}$  and  $\mathbf{1}_{\text{Me}}$  without solvent effects. Currently, the inclusion of solvent effect on the optical spectra is not included in GPAW. Figure S5 gives the overlay of  $\mathbf{1}$  and  $\mathbf{1}_{\text{Me}}$ . It should be noted that the optical transitions of  $\mathbf{1}$  could not be clearly determined. The inclusion of the full ligand introduces hundreds of additional states. However, through the reduction of the ligand, the number of states is reduced. However, the optical spectra for  $\mathbf{1}$  and  $\mathbf{1}_{\text{Me}}$  qualitatively agree (Figure S5).

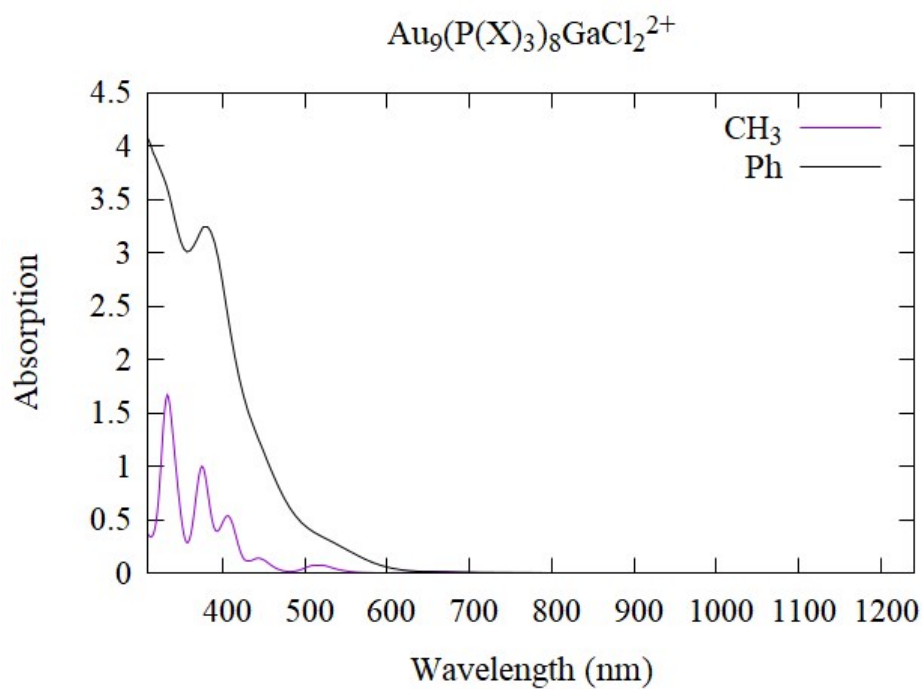


## 5. Detailed View of $[(PPh_3)_8Au_9GaCl_2]^{2+}$ and $[(PMe_3)_8Au_9GaCl_2]^{2+}$

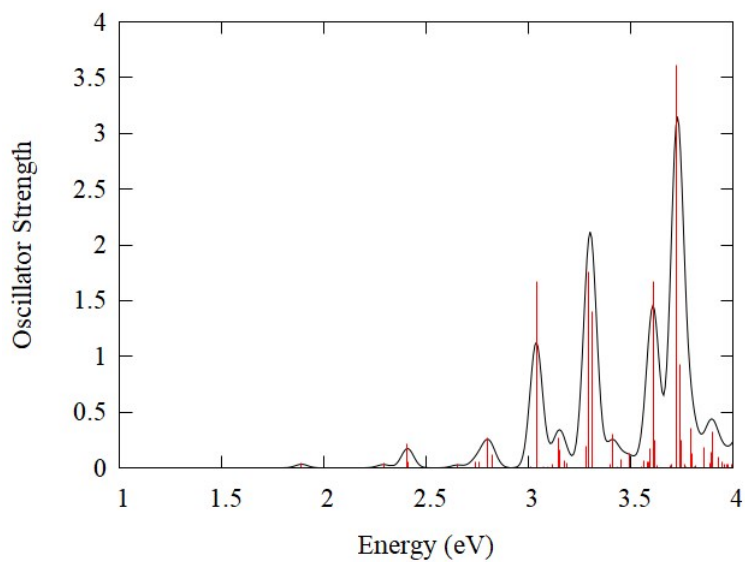


**Figure S4:** Ball and stick representation of the complete molecular structure of  $Cu_6(SC_7H_4NO)_6 [(PPh_3)_8Au_9GaCl_2]^{2+}$  and  $[(PMe_3)_8Au_9GaCl_2]^{2+}$ . The gold, purple, blue, black, white, and green balls represent the Au, P, Ga, C, H, and Cl atoms respectively.

## 6. Optical spectra of **1** and **1<sub>Me</sub>**.



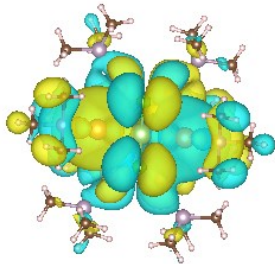
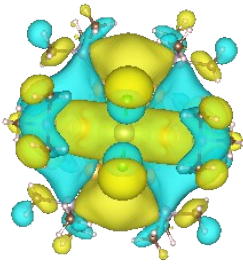
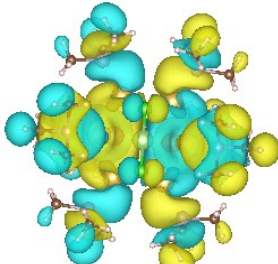
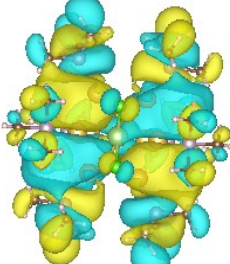
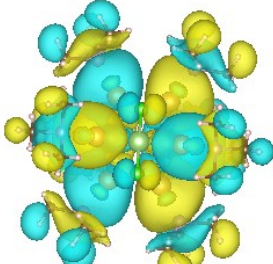
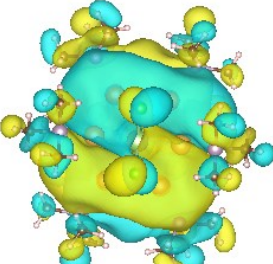
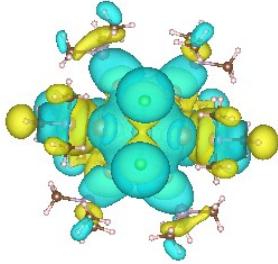
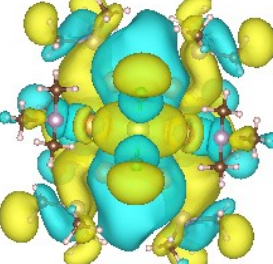
**Figure S5.** The theoretical UV-Vis spectrum of **1** (black line) in comparison to the UV-Vis spectrum of **1<sub>Me</sub>** (purple line).



**Figure S6.** The theoretical UV-Vis spectrum of **1<sub>Me</sub>** in eV with sticks representing specific transitions.

## 7. Electron density corresponding to optical transitions

**Table S2.** Kohn-Sham electron density orbitals corresponding to the simulated electronic transitions for the UV-Vis spectra. The transitions are given in both electron volts and nanometers.

eV/nm	From	To
3.038/408		
	HOMO-6	LUMO
3.148/394		
	HOMO-2	LUMO+3
3.151/393		
	HOMO-3	LUMO+2
3.313/374		
	HOMO-1	LUMO+4

## 8. TGA measurements

Thermogravimetical analysis of **1** is displayed in Figure SX. It shows a loss of mass of 55.27% which is in good accordance with the calculated value of 56.4%. The remaining mass consists of the remaining metals gold and gallium.

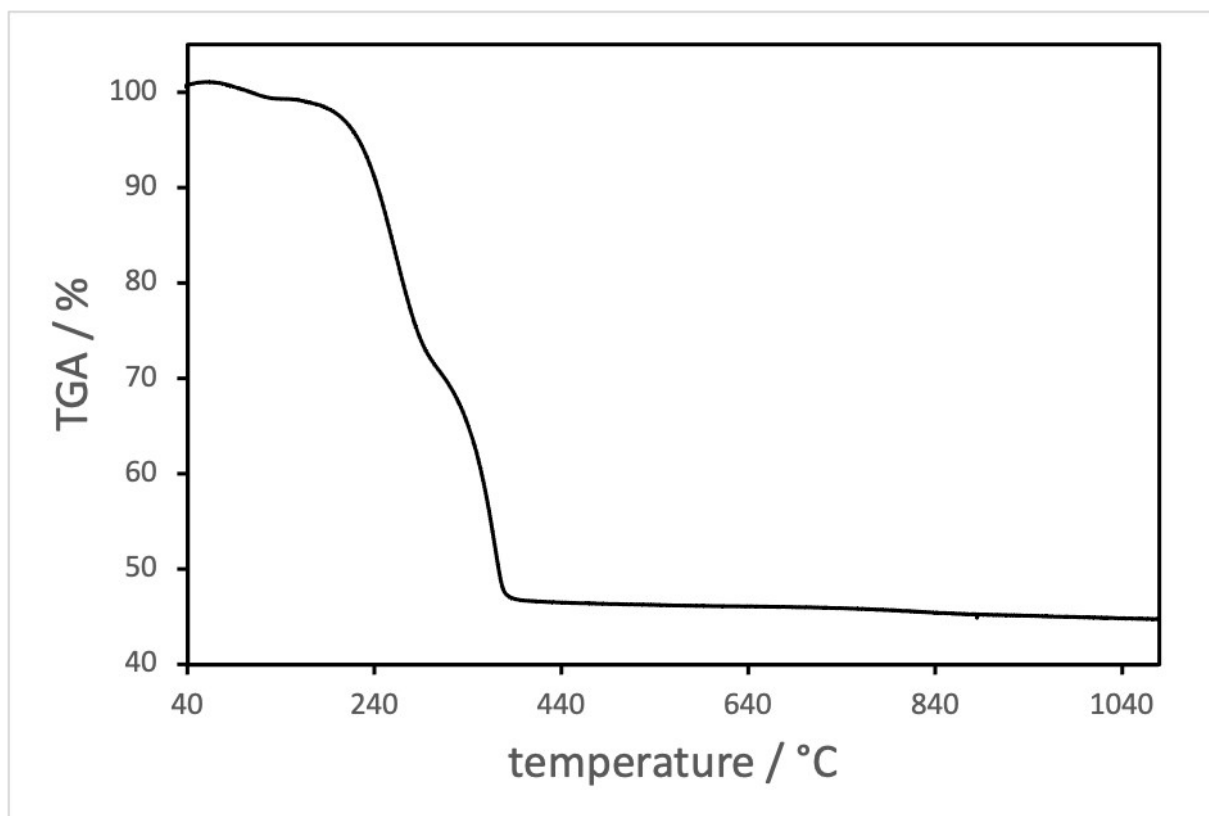


**Figure S7:** Thermogravimetical analysis of  $[(\text{PPh}_3)_8\text{Au}_9\text{GaCl}_2]^{2+}(\text{GaCl}_4)_{1.25}(\text{GaCl}_3\text{Cp})_{0.75}$ . The initial increase is caused by measurement procedure followed by the evaporation of solvent trapped in the crystals. The total loss of mass of 55.2% suits the theoretical loss of mass of 56.4%.

## 9. HR-ESI-MS spectra

Figures S8-S12 show the high resolution spectra compounds which could be identified in the ESI-MS measurement including the title compound **1**.

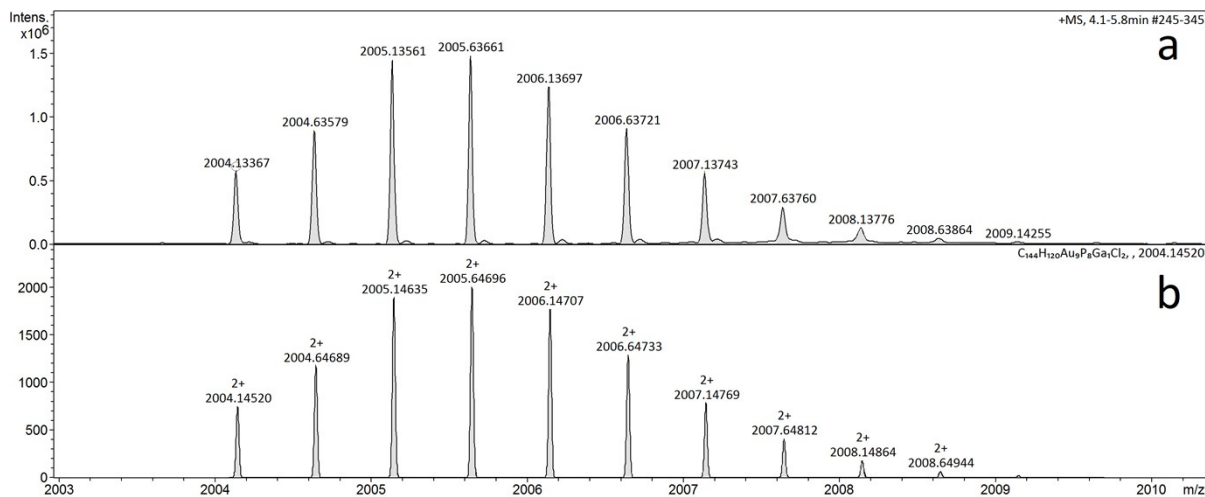


Figure S8: HR-ESI mass spectrum of the title compound  $[\text{Au}_9(\text{PPh}_3)_8\text{GaCl}_2]^{2+}$  including the measured high-resolution spectrum (a) and the calculated peaks (b)

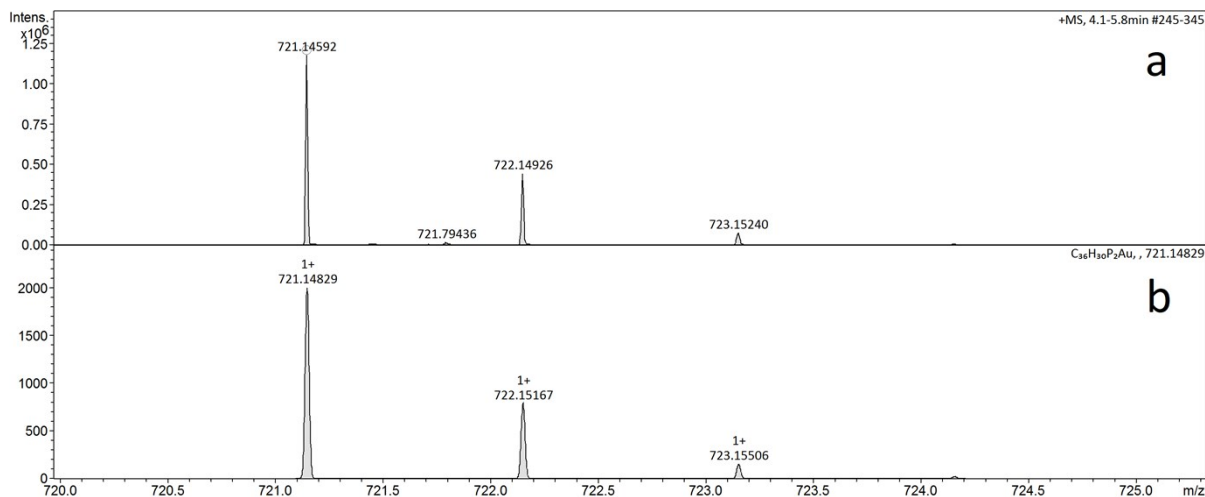


Figure S9: HR-ESI mass spectrum of  $[\text{Au}(\text{PPh}_3)_2]^+$  including the measured high-resolution spectrum (a) and the calculated peaks (b)

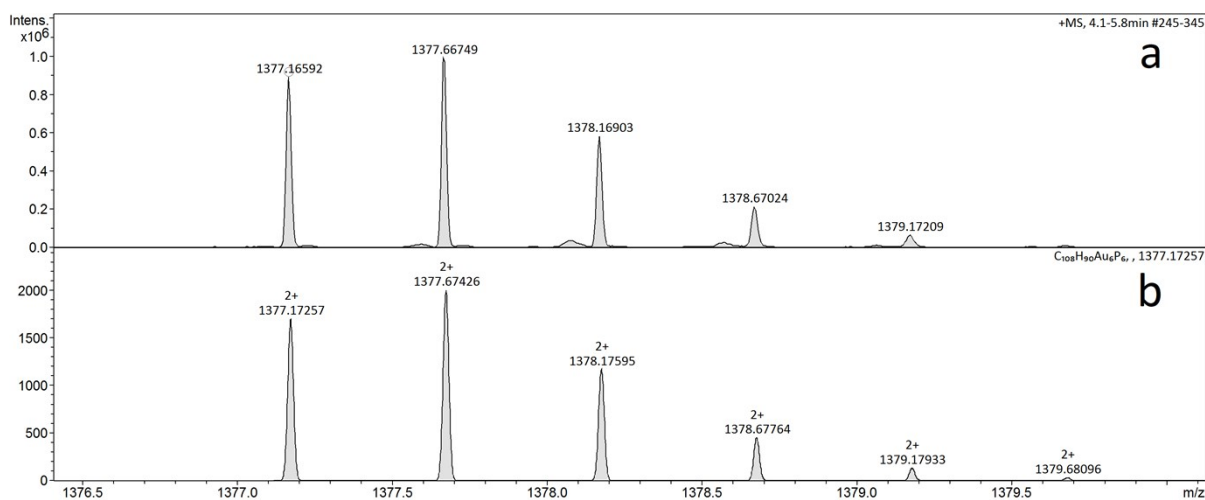


Figure S10: HR-ESI mass spectrum of  $[\text{Au}_6(\text{PPh}_3)_6]^{2+}$  including the measured high-resolution spectrum (a) and the calculated peaks (b)

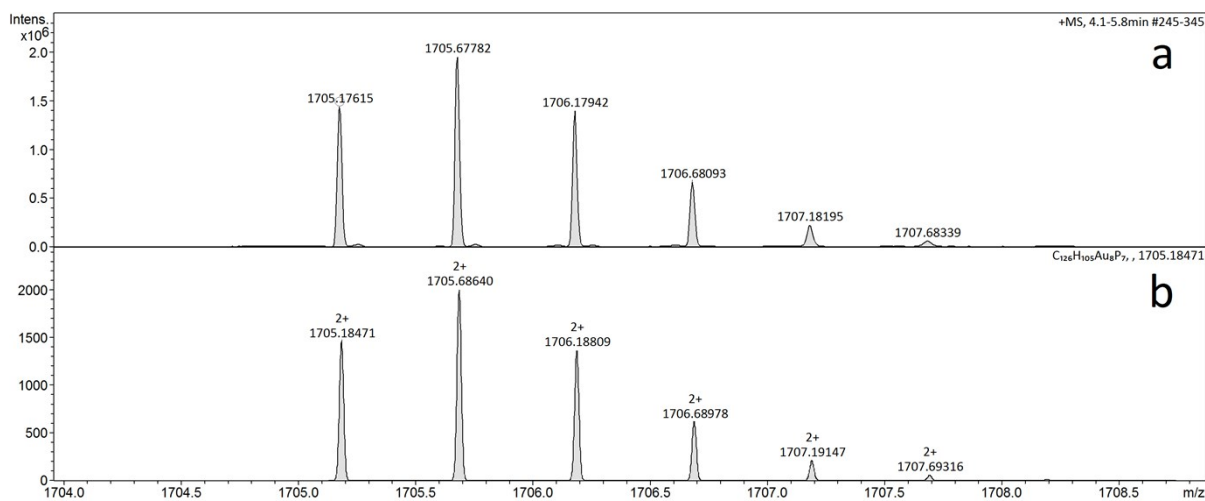


Figure S11: HR-ESI mass spectrum of  $[\text{Au}_8(\text{PPh}_3)_7]^{2+}$  including the measured high-resolution spectrum (a) and the calculated peaks (b)

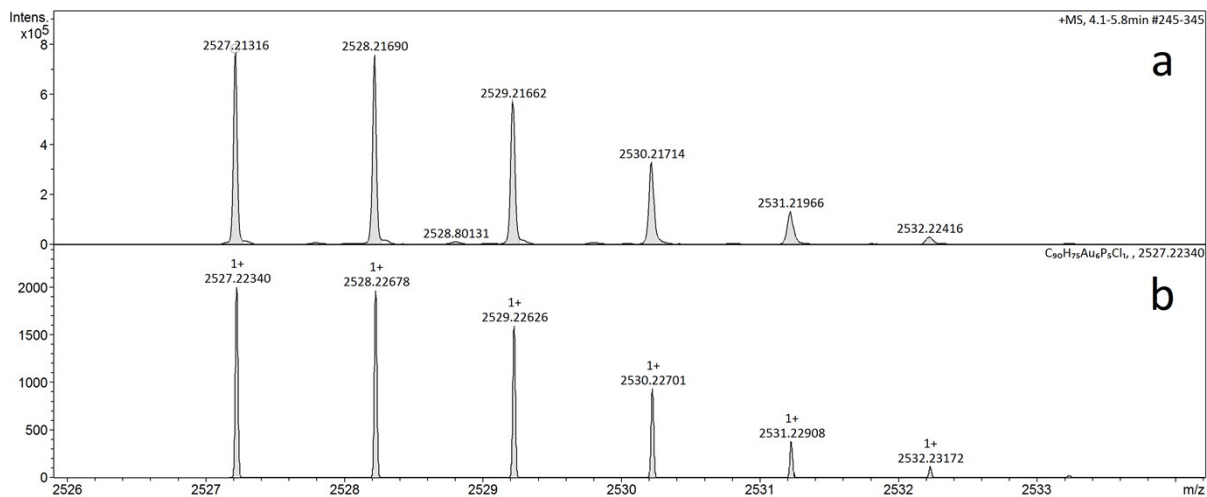


Figure S12: HR-ESI mass spectrum of  $[\text{Au}_6(\text{PPh}_3)_5\text{Cl}]^+$  including the measured spectrum (a) and the calculated peaks (b)

## References:

- 
- [1] C. Schenk, R. Köppe, H. Schnöckel, A. Schnepf, *Eur. J. Inorg. Chem.* **2011**, 25, 3681-3685.
- [2] (a) G. M. Sheldrick, *Acta Crystallogr.* **2008**, A64, 112–122; (b) G. M. Sheldrick, *Acta Crystallogr., Sect. C: Struct. Chem.* **2015**, C71, 3–8.
- [3] O. V. Dolomanov, L. J. Bourhis, R. J. Gildea, J. A. K. Howard, H. Puschmann, *J. Appl. Crystallogr.* **2009**, 42, 339–341.
- [4] A. L. Spek, *Acta Cryst.* **2009**, D65, 148 - 155.
- [5] (a) J. J. Mortensen, L. B. Hansen, and K. W. Jacobsen, *Phys. Rev. B*, **2005**, 71, 035109; (b) J. Enkovaara, C. Rostgaard, J. J. Mortensen et al., *J. Phys.: Condens. Matter.*, **2010**, 22, 253202, (c) A. H. Larsen, J. J. Mortensen, J. Blomqvist, I. E. Castelli, et al., *J. Phys.: Condens. Matter.*, **2017**, 29, 273002.
- [6] Perdew, J. P.; Burke, K.; Ernzerhof, M. *Phys. Rev. Lett.* **1996**, 77 (18), 3865–3868.
- [7] K. Momma, F. Izumi, *J. Appl. Crystallogr.* **2008**, 41, 653–658.
- [8] M. Walter, H. Häkkinen, L. Lehtovaara, M. Puska, J. Enkovaara, C. Rostgaard and J. J. Mortensen, *J. Chem. Phys.*, **2008**, 128, 244101.